iScience

CellPress

Article

A Novel Neuroprotective Role of *Phosphatase of Regenerating Liver-1* against CO_2 Stimulation in *Drosophila*

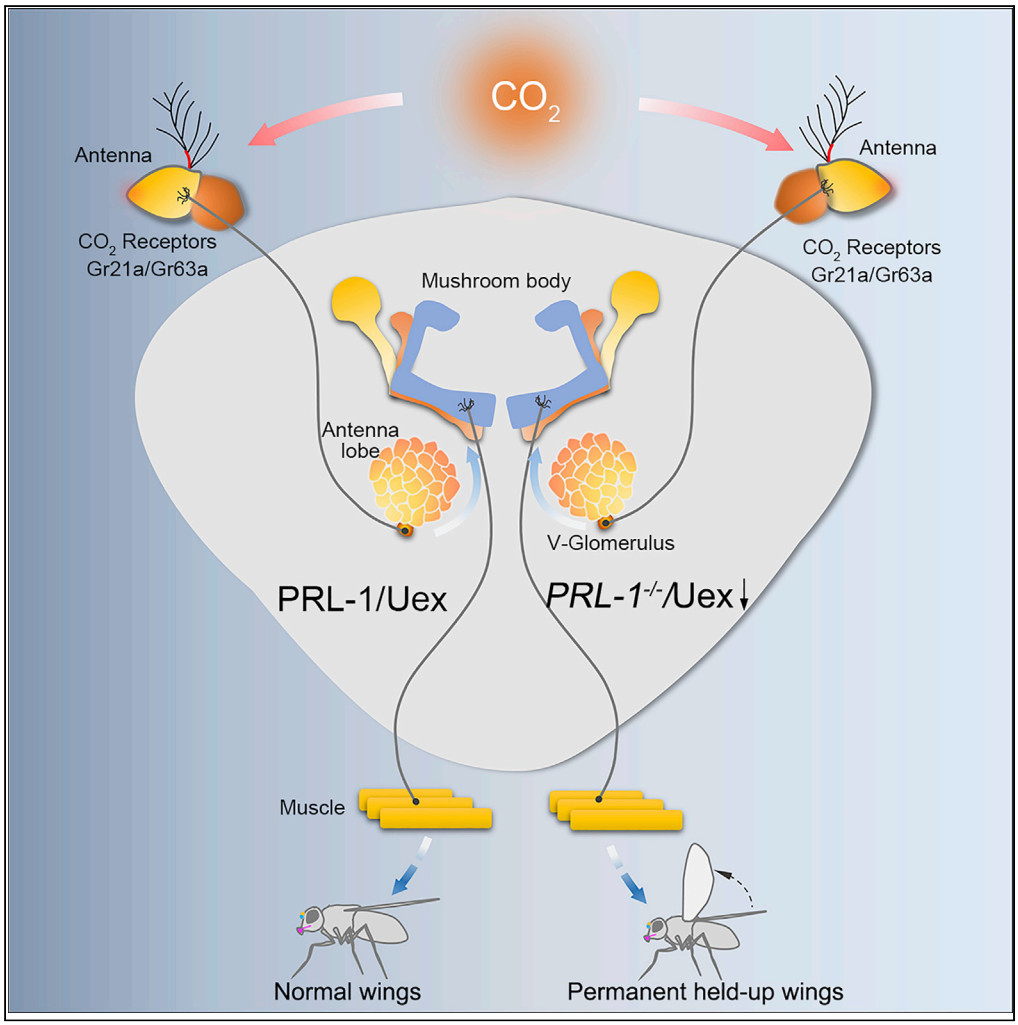

Pengfei Guo, Xiao Xu, Fang Wang, ..., Zhefeng Gong, Xiaohang Yang, Yongmei Xi

xhyang@zju.edu.cn (X.Y.)
xyyongm@zju.edu.cn (Y.X.)

HIGHLIGHTS

PRL-1 functions to protect the nervous system against olfactory CO_2 stimulation

PRL-1 physically interacts with Uex and controls Uex expression levels

PRLs may retain a similar neuroprotective function in humans

Guo et al., iScience *19*, 291–302
September 27, 2019 © 2019 The Author(s).
https://doi.org/10.1016/j.isci.2019.07.026

iScience

CellPress

Article

A Novel Neuroprotective Role of *Phosphatase of Regenerating Liver-1* against CO_2 Stimulation in *Drosophila*

Pengfei Guo,[1,2,6] Xiao Xu,[1,2,6] Fang Wang,[2] Xin Yuan,[1] Yinqi Tu,[1,2] Bei Zhang,[1,2] Huimei Zheng,[1] Danqing Yu,[3] Wanzhong Ge,[1] Zhefeng Gong,[4] Xiaohang Yang,[1,5,*] and Yongmei Xi[1,7,*]

SUMMARY

Neuroprotection is essential for the maintenance of normal physiological functions in the nervous system. This is especially true under stress conditions. Here, we demonstrate a novel protective function of PRL-1 against CO_2 stimulation in *Drosophila*. In the absence of PRL-1, flies exhibit a permanent held-up wing phenotype upon CO_2 exposure. Knockdown of the CO_2 olfactory receptor, Gr21a, suppresses the phenotype. Our genetic data indicate that the wing phenotype is due to a neural dysfunction. PRL-1 physically interacts with Uex and controls Uex expression levels. Knockdown of Uex alone leads to a similar wing held-up phenotype to that of *PRL-1* mutants. Uex acts downstream of PRL-1. Elevated Uex levels in *PRL-1* mutants prevent the CO_2-induced phenotype. PRL-1 and Uex are required for a wide range of neurons to maintain neuroprotective functions. Expression of human homologs of PRL-1 could rescue the phenotype in *Drosophila*, suggesting a similar function in humans.

INTRODUCTION

The mammalian phosphatase of regenerating liver (PRL) family contains three members, PRL-1, PRL-2, and PRL-3 (Diamond et al., 1994; Zeng et al., 1998). Human PRLs have been implicated in multiple cancers (Bessette et al., 2008; Campbell and Zhang, 2014; Saha et al., 2001; Al-Aidaroos and Zeng, 2010). The PRL expression patterns in several animal models have been characterized. In *Drosophila*, amphioxus, and zebrafish, PRL family members have been detected in many tissues including those of the central nervous system (CNS) during embryonic development (Pagarigan et al., 2013; Lin et al., 2013). In mice, mPRL-2 is expressed ubiquitously in the hippocampal pyramidal neurons, ependymal cells, and cone and rod photoreceptor cells (Gungabeesoon et al., 2016). An early study of rat brains demonstrated that the expression of PRL in neurons and oligodendrocytes was enhanced in the cerebral cortex following transient forebrain ischemia (Takano et al., 1996). In *Drosophila*, PRL-1 is the only homolog of mammalian PRLs. The exact physiological functions of the PRLs remain largely unknown.

CO_2-evoked behavioral responses in many winged insects are important for food foraging, reproduction, and survival (Guerenstein et al., 2004; McMeniman et al., 2014; Stange and Stowe, 1999). CO_2 as a natural gas is odorless for humans, although CO_2-responsive neurons do exist (Shusterman and Avila, 2003; Ji et al., 2007). *Drosophila* is highly sensitive to CO_2, and the sensing of CO_2 is usually accompanied by immediate physiological and behavioral responses. These responses have been previously studied mainly in terms of anesthetic and toxic effects under high concentrations of CO_2 (Dijken et al., 1977; Badre et al., 2005). When using standard CO_2 anesthetic protocol in fly work, *wt* adult flies respond with a brief loss of motion and activity and subsequently develop a held-up wing phenotype under extended exposure to a high concentration of CO_2. These flies recover normal wing function and return to normal activity levels upon the resumption of normal atmospheric levels of CO_2.

CO_2 also acts as an unfavorable stress odorant eliciting avoidance behavior in *Drosophila* (Suh et al., 2004). It has been reported that such avoidance behavior is mediated by the CO_2 receptors Gr21a and Gr63a that function together as a heterodimer (Scott et al., 2001; Jones et al., 2007). These chemosensory receptors are specifically expressed in CO_2-responsive neurons harbored in the third segment of the antennae (Scott et al., 2001; Jones et al., 2007). In the sensilla of the antenna, olfactory receptor neurons (ORNs) send their axonal projections into the antennal lobe (AL) to form glomeruli. It is these glomeruli that act as the primary olfactory center of the brain (Couto et al., 2005). The stereotyped V-glomerulus in the most ventral AL is

[1]Institute of Genetics and Department of Genetics, Division of Human Reproduction and Developmental Genetics of the Women's Hospital, Zhejiang University School of Medicine, Yuhangtang Road 866, Xihu District, Hangzhou, Zhejiang Province 310058, China

[2]College of Life Sciences, Zhejiang University, Yuhangtang Road 866, Xihu District, Hangzhou, Zhejiang Province 310058, China

[3]The Second Affiliated Hospital, Zhejiang University School of Medicine, Yuhangtang Road 866, Xihu District, Hangzhou, Zhejiang Province 310058, China

[4]Department of Neurobiology, Key Laboratory of Medical Neurobiology of the Ministry of Health of China, Key Laboratory of Neurobiology, Zhejiang University School of Medicine, Yuhangtang Road 866, Xihu District, Hangzhou, Zhejiang Province 310058, China

[5]Joint Institute of Genetics and Genomic Medicine between Zhejiang University and University of Toronto, Zhejiang University, Hangzhou, Zhejiang Province 310058, China

[6]These authors contributed equally

[7]Lead Contact

*Correspondence: xhyang@zju.edu.cn (X.Y.), xyyongm@zju.edu.cn (Y.X.)

https://doi.org/10.1016/j.isci.2019.07.026

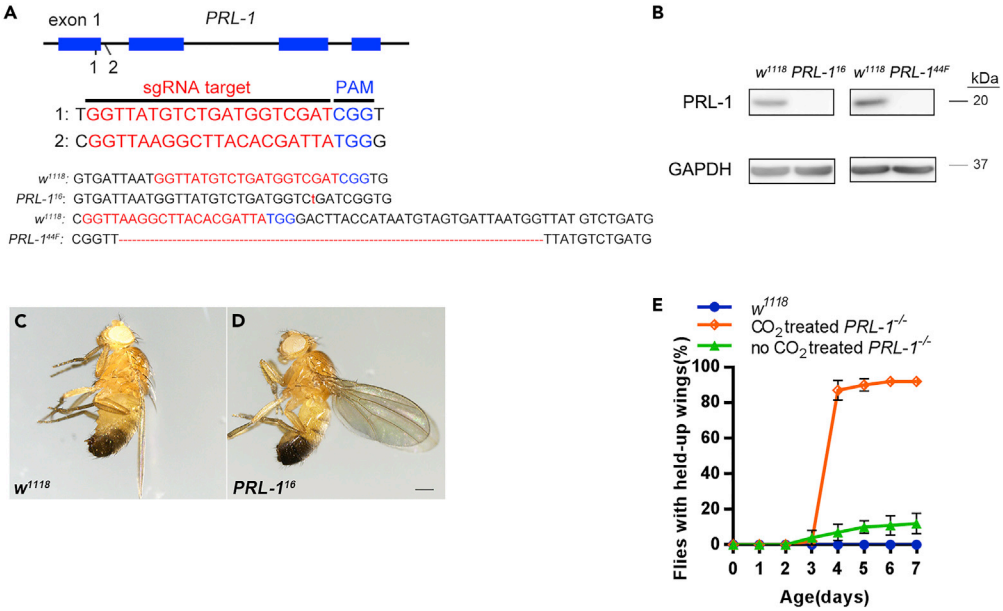

Figure 1. Absence of PRL-1 Leads to CO_2-Induced Wing Phenotype

(A) Two independent frameshift mutant alleles, *PRL-1*^{16} and *PRl-1*^{44F}, were generated with the CRISPR/Cas9 method. The targets of *PRL-1* guide RNA (gRNA) were located in the first exon and nearby intron separately. Target 1 produced a site mutation, which added one base pair into the gRNA sequence. Target 2 produced a much longer genomic DNA deletion, which removed 51 bp near the gRNA sequence. Both of these targets caused a stop code in the following sequence, terminating translation after the 35th (*PRL-1*^{16}) or 49th (*PRL-1*^{44F}) amino acid residue.

(B) Western blot analyses of mutant flies. Lysates were probed with anti-PRL-1 and anti-GAPDH antibodies.

(C and D) *PRL-1* mutant flies exhibited a permanent wing held-up phenotype upon CO_2 stimulation (D), compared to *wt* flies under the same condition (C). Scale bar, 25 μm.

(E) Statistical calculations of fly populations with wing held-up phenotype. About 90% of 3-day-old male *PRL-1* mutant animals displayed a permanent wing held-up phenotype upon CO_2 exposure within 24 h (orange). A low background of spontaneous wing phenotype was also detected in the mutant flies in the ambient environment (green).

Data are expressed as mean ± SD. See also Figure S1.

responsive to CO_2 stimuli. It then conveys the signals to the mushroom body (MB) as a higher processing center (Sachse et al., 2007; Vosshall and Stocker, 2007). Eventually, the nervous system translates the processed olfactory signals into animal behavior.

In this study we found that in the absence of PRL-1, the adult flies treated with high concentrations of CO_2 exhibited a permanent wing held-up phenotype that failed to recover in the ambient environment. The deprivation of the CO_2 chemosensory receptor protein Gr21a or the overexpression of PRL-1 in the nervous system was able to suppress the wing phenotype in mutant animals. In addition, we found that PRL-1 interacted with Unextended wing (*uex*) and regulated its expression. The down-regulation of Uex alone resulted in the same wing held-up phenotype and elevated Uex levels in *PRL-1* mutants to prevent the wing phenotype induced by CO_2. Expression of human homologs of PRL-1 could rescue the phenotype in *Drosophila*. Our data demonstrate a novel function of PRL-1 in preventing neural dysfunction from CO_2 insult and shed light on the understanding of hPRL functions in human diseases.

RESULTS

Absence of PRL-1 Leads to CO_2-Induced Wing Phenotype

To search for potential physiological functions of the hPRLs, we took advantage of the simplicity of the *Drosophila* genome. Two independent mutant isolates of *PRL-1* were generated with the CRISPR/Cas9 method (Bassett et al., 2013; Bassett and Liu, 2014). Both lines turned out to be frameshift mutations and caused a stop codon-terminating translation after 35 (*PRL-1*^{16}) or 49 (*PRL-1*^{44F}) amino acid residues (Figure 1A). These two alleles were viable and developed into morphologically normal adults. Western blot analyses with the antibody against full-length amino acid sequence of PRL-1 exhibited an obvious

band of 20 kDa in *wt* flies, but not in the mutants (Figure 1B), suggesting that mutant lines were loss-of-function alleles. As both isolates were null alleles, we only employed the *PRL-1*^{16} mutant (referred to as *PRL-1*$^{-/-}$ *or PRL-1* mutant) in this study.

It appeared that PRL-1 was not critical for animal development and survival. One of the possibilities was that PRL-1 was involved primarily in stress responses. We interrogated mutant adult flies with various stress stimuli, including ultraviolet, X-ray, cold, heat, starvation, and CO_2. Interestingly, only high concentration of CO_2 treatment (a pulse of 5 L/min CO_2 for 20 s in a vial with a plug) caused a vertical held-up wing phenotype in *PRL-1* mutant flies within 24 h after CO_2 exposure (Figure 1D), whereas *wt* control flies did not show any such response (Figure 1C). Further study found that young flies, 3 days after eclosion, were most responsive to such CO_2 exposure, with about 90% of such flies displaying the held-up wing phenotype (Figures 1E and S1A). We also detected a low background of spontaneous held-up wing phenotype in the *PRL-1* mutant flies in the ambient environment (Figure 1E). It appeared that the male animals displayed the more prominent wing phenotype than the females (Figure S1B). We therefore only focused on male responses in the following experiments. We monitored the wing held-up phenotype in *PRL-1* mutant flies induced by CO_2 exposure over time and found that this wing phenotype was permanent (Figure 1E). The lifespan of the mutant flies with this wing phenotype remained the same as that of the *wt* animals, despite their inability to fly (Figure S1C).

Wing Phenotype Is Rescued by PRL-1 Expression in the Nervous System

It was clear that the wing held-up wing phenotype could be either caused by a defect of the nervous system or a dysfunction of the wing muscles in the absence of PRL-1. To address this issue, we employed genetic approaches to identify the tissue in which PRL-1 expression could rescue the wing phenotype. PRL-1 expression in the mutant background was driven by an array of tissue-specific *GAL4* lines. Our data showed that only the pan-neuronal expression (*elav-GAL4*) of PRL-1 completely prevented the wing phenotype induced by CO_2 exposure (Figure 2A). Neither the muscle-specific (*Mhc-GAL4*) nor the glial (*repo-GAL4*) expression of PRL-1 had any rescue effect (Figure 2A). Examination of the indirect flight muscles by phalloidin staining and transmission electrical microscopy showed no obvious differences between the *wt* and the mutants (Figures S2A and 2B). Based on these observations we conclude that PRL-1 plays an important protective role in the nervous system. The held-up wing phenotype induced by CO_2 exposure was caused by a defective neuronal function occurring in the absence of PRL-1.

We also explored the possibility whether human homologs of PRLs could rescue the wing phenotype. Two human homologs, hPRL-1 and hPRL-2, were tested. Either of them fulfilled *Drosophila* PRL-1 function and was able to effectively rescue the wing phenotype (Figure S1D). This result implies that hPRLs may have a similar role in humans.

CO_2 Sensory Circuitry Is Required for the Wing Phenotype

Our data indicated that PRL-1 plays a protective role in the nervous system. However, the permanent held-up wing phenotype could simply be due to the depletion of O_2 during the CO_2 exposure. To test this possibility, N_2 was used to anesthetize mutant flies, and no held-up wing phenotype was observed (Figure 2B), suggesting that the wing phenotype was not caused by the lack of O_2. In addition, ether was used to test whether anesthesia alone could cause the wing phenotype, and, again, such a positive correlation did not occur (Figure 2B).

Analysis of CO_2-evoked avoidance behavior using T-maze assays (Kwon et al., 2007; Suh et al., 2004) revealed no significant differences between *PRL-1* mutants and the *wt* animals (Figure S4A). This indicates that the olfactory sensing of CO_2 remains active in the *PRL-1* mutants. To further exclude the possibility that it was pH changes in body fluid, occurring through the trachea via exposure to the high concentration of CO_2 that may have led to the wing phenotype, we blocked CO_2 sensory circuitry in mutant flies. As most of the double mutant flies bearing either *Gr21a* or *Gr63a* with the *PRL-1* mutation died at the pupal stage, we employed RNA interference (RNAi) method to specifically knock down Gr21a in the CO_2-responsive neurons. *PRL-1* mutant flies carrying *Gr63a-GAL4>Gr21a-RNAi* no longer displayed any wing held-up wing phenotype upon CO_2 exposure (Figure 2C). This observation indicates that it is the signals generated by CO_2-responsive neurons that trigger the characteristic wing phenotype in the *PRL-1* mutants. It is therefore unlikely that any pH change in body fluid has played a role in this event.

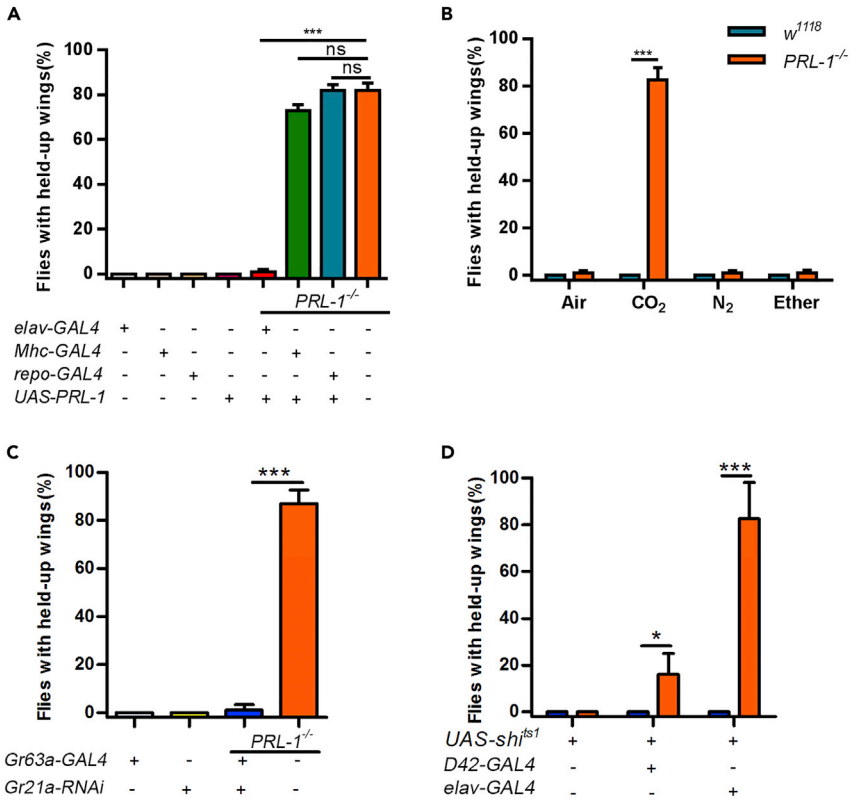

Figure 2. Statistical Data Showed Protective Role of PRL-1 in Nervous System against CO_2 Insult

(A) Neuronal-specific expression of PRL-1 (*elav-GAL4*) in the mutants completely rescued the wing held-up phenotype induced by CO_2, but expression in other tissues such as muscles (*Mhc-GAL4*) or glial cells (*repo-GAL4*) did not result in any rescue.

(B) The response of *PRL-1* mutant flies to alternative anesthetics, such as carbon dioxide (CO_2), ether, and nitrogen (N_2). Permanent wing phenotype was only induced by CO_2.

(C) In the *PRL-1* mutant background, knockdown of CO_2 sensory receptor protein Gr21a driven by *Gr63a-GAL4* prevented the wing phenotype.

(D) Within the transition time (about 10 min) when flies were shifted from non-permissive temperature (29°C) back to the permissive temperature (25°C), the vast majority of flies ectopically expressed shi^{ts1} in the nervous system (*elav-GAL4>UAS-*shi^{ts1}) and exhibited a transient wing held-up phenotype. A similar wing phenotype was also observed when $shi^{ts1}$was specifically expressed in motor neurons (*D42-GAL4>UAS-*shi^{ts1}).

Data are expressed as mean ± SD. *p < 0.05, ***p < 0.001. See also Figures S2 and S4.

Held-up Wing Phenotype Is due to Neural Dysfunction

To further confirm that it was neural dysfunction that caused wing phenotype, we took advantage of a temperature-sensitive shi^{ts1} allele. In this, at a non-permissive temperature (29°C), the synaptic vesicle recycling is halted and neuronal transmission is blocked (Kosaka and Ikeda, 2010; Kitamoto, 2001). As expected, at 29°C the flies (*elav-GAL4>UAS-*shi^{ts1}) were paralyzed. When the flies were shifted back from non-permissive temperature to the permissive temperature (29°C–25°C), the vast majority of flies with shi^{ts1} in the nervous system exhibited a transient held-up wing phenotype within the recovery time (about 10 min) (Figures 2D and S4B), which was reminiscent of that observed in *PRL-1* mutant flies induced by CO_2 exposure (Figure 1D). We also observed a similar wing phenotype when $shi^{ts1}$was expressed in motor neurons (*D42-GAL4>UAS-*shi^{ts1}) (Figure 2D). The same held-up wing phenotype also appeared during the temperature shift from 25°C to 29°C.

It is reasonable to assume that the synaptic vesicle recycling in *elav-GAL4>UAS-*shi^{ts1} flies is not fully functional and that neurotransmission is affected within the transition time from 29°C to 25°C. Therefore the held-up wing phenotype is most likely due to neural dysfunction. Our data suggest that it was the neurotransmission defects in a wide range of neurons, including motor neurons, that were responsible for the wing phenotype. Based on these observations, we conclude that the CO_2-induced held-up wing phenotype in *PRL-1* mutant flies is due to neural dysfunction.

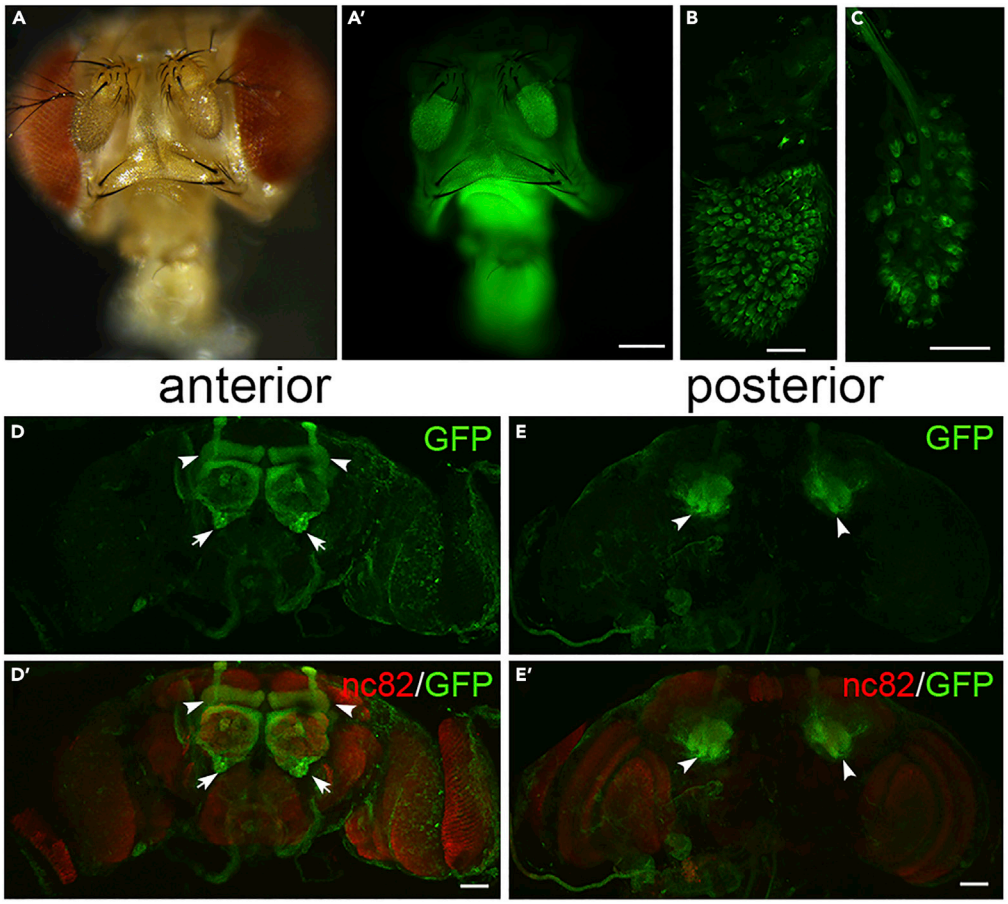

Figure 3. PRL-1 Is Expressed in the CO_2 Sensory Circuitry

Images of the expression pattern of *EGFP-PRL-1* driven by *PRL-GAL4*.

(A and A′) GFP fluorescence signals in the adult head.

(B and C) Confocal scanning of the antennae (B) and maxillary palps (C) shows the expression of PRL-1 in the basiconic sensilla.

(D–E′) Immunofluorescence staining reveals the spatial expression of *UAS-EGFP-PRL-1* driven by *PRL-GAL4* in the anterior (D and D′) and posterior parts (E and E′) of the brain. The brains were double labeled with anti-GFP (green) and anti-nc82 (red). The distribution of PRL-GAL4 was strong in the V-glomeruli (arrows) and mushroom body (arrowheads).

Scale bar, 30 μm in (B–E′) and 39 μm in (A′). See also Figure S3.

PRL-1 Is Expressed in the CO_2 Sensory Neural Circuitry

PRL-1 expression was detected in the adult head by western blot (Figure S4C). We stained the adult brains with anti-PRL-1 antibodies. PRL-1 was detected in the AL including the V-glomeruli (Figures S3B–S3B″). As a control, these PRL-1 signals were not detectable in the *PRL-1* mutant brains (Figures S3C–S3C″). To visualize the PRL-1 expressing neurons, we generated *PRL-1-GAL4* transgenic flies with a 6.1-kb genomic DNA fragment immediately 5′ of the ATG codon of the *PRL-1* gene. The GFP signals were robust in the head, the third segment of antennae, and the maxillary palp (Figures 3A and 3A′). Confocal images showed an obvious distribution of PRL-1 in the basiconic sensilla (Figures 3B and 3C), which harbors the cell bodies of ORNs, including those of CO_2-responsive neurons (Scott et al., 2001; Suh et al., 2004). The strong GFP signals were observed in the V-glomeruli (arrows, Figures 3D and 3D′), as well as the MB (arrow heads, Figures 3D–3E′). The signals of *EGFP-PRL-1* driven by *PRL-1-GAL4* and anti-PRL-1 antibody staining were both observed in the CO_2 neural circuitry (Figures 3D–3D′ and S3A–3A″).

CO_2 Triggers Hyperactive Ca^{2+} Activity in the Antennal Lobe of the *PRL-1* Mutant Brain

To analyze the PRL-1 function in the brain, we estimated the neuronal activity with calcium-sensitive fluorescent protein (GCaMP) (Jones et al., 2007; Wang et al., 2003). It is known that the neurons in the

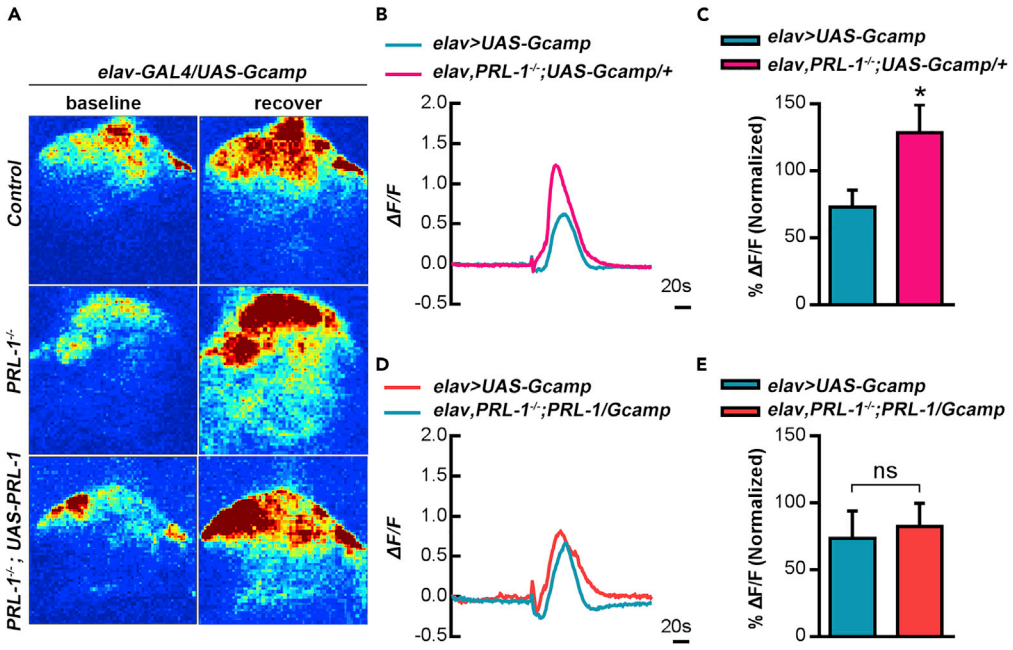

Figure 4. CO_2 Triggers Hyperactive Ca^{2+} Activity in the Antennal Lobe of the *PRL-1* Mutant Brain

(A) Calcium activity in the antennal lobes of control, *PRL-1* mutant, or *PRL-1*-rescued flies with CO_2 stimulation. Representative images of GCaMP6.0 fluorescence were obtained from living imaging at the baseline and after CO_2 stimuli (%ΔF/F).

(B and C) The magnitude of GCaMP signal changes in *PRL-1* mutant brains was about 2-fold that of the controls (average peak ΔF/F of *PRL-1* mutants is 1.21 ± 0.51; average peak ΔF/F of WT is 0.55 ± 0.46) (B), also shown in the bar graph quantitation (C).

(D and E) The overexpression of a *UAS-PRL-1* transgene driven by *elav-GAL4* in the mutants could restore CO_2-evoked Ca^{2+} sensitivity (D), also shown in the bar graph quantitation (E).

Statistics for (C) and (E): Data are expressed as mean ± SD. Two-tailed Student's t test with *p < 0.05, ns, not significant. n = 6 for each group.

V-glomeruli of the AL respond to CO_2 stimuli (Jones et al., 2007). We examined the transient Ca^{2+}signals triggered by CO_2 in the AL region of the brain in living flies. Upon 20-s CO_2 exposure, the GCaMP signals in *wt* and mutant brains were recorded and analyzed (Figure 4A). The magnitude of GCaMP signal changes in *PRL-1* mutant brains was about 2-fold of those of the controls (average peak ΔF/F of *PRL-1* mutants: 1.21 ± 0.51; average peak ΔF/F of *wt*: 0.55 ± 0.46) (Figures 4B and 4C). The overexpression of a *UAS-PRL-1* transgene driven by *elav-GAL4* in the mutants could restore CO_2-evoked Ca^{2+} sensitivity (Figures 4D and 4E). This result suggests that, in the absence of PRL-1, the neurons in the AL, including those of the V-glomeruli, are hyperactive upon CO_2 stimulation. This phenomenon may unveil neural dysfunction in the nervous system of the mutant.

Uex Knockdown Results in an Identical Held-up Wing Phenotype

We next asked if any genes downstream of PRL-1 are involved in the wing held-up phenotype. It was reported that cyclin M/ancient conserved domain proteins (CNNMs) interacted with hPRL-1 or hPRL-2 during cancer metastasis (Funato et al., 2014; Hardy et al., 2015). We examined whether PRL-1 also interacted with Uex, the only *Drosophila* homolog of human CNNMs. S2 cells were transfected with PRL-1 tagged with 3xHA at the N terminus. Cell lysates were subjected to immunoprecipitation with an anti-hemagglutinin antibody and analyzed by western blot with the anti-Uex. In this assay, endogenous Uex was co-immunoprecipitated by PRL-1 (Figure 5A). We performed a biotin pull-down experiment to confirm the interaction between PRL-1 and Uex (Figure S5A). A glutathione S-transferase (GST)-pull-down assay validated the direct interaction between PRL-1 and Uex (Figure 5B). The co-localization of PRL-1 and Uex on the plasma membrane of S2 cells was also detected by double-immunofluorescence staining with the antibodies against PRL-1 and Uex (Figure 5D).

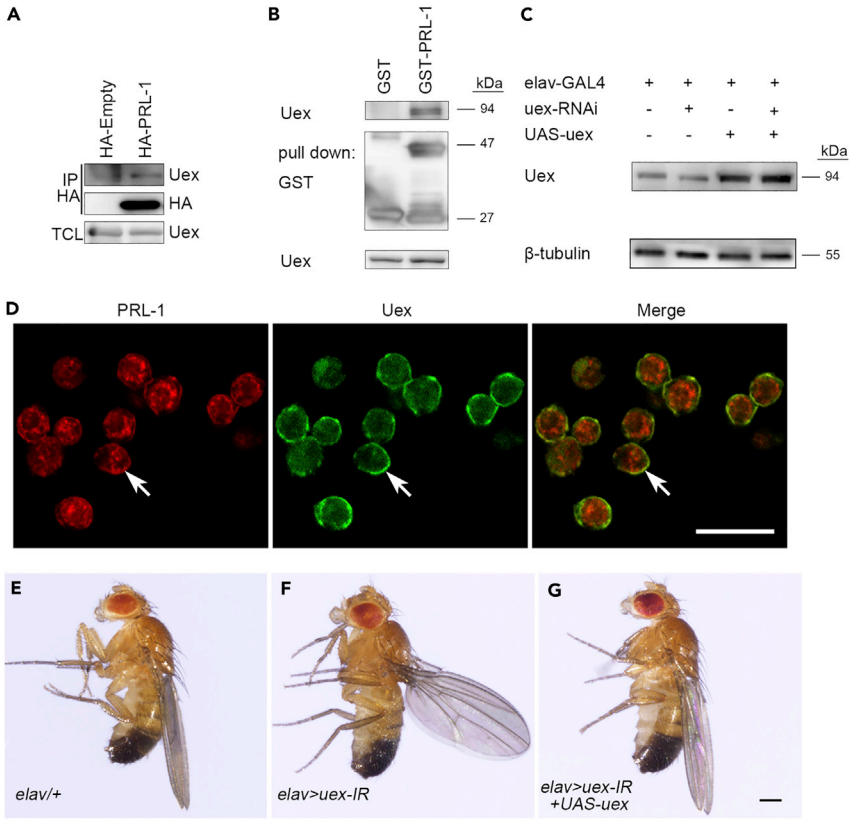

Figure 5. Uex Knockdown Results in an Identical Wing Held-up Phenotype

(A) Coimmunoprecipitation analysis with transient transfection of either empty or hemagglutinin (HA)-tagged PRL-1 in S2 cells showed that Uex was co-immunoprecipitated with PRL-1.

(B) *In vitro* glutathione S-transferase (GST) pull-down assay with purified GST-tagged PRL-1 confirmed a direct interaction between Uex and PRL-1.

(C) Western blot with brain extracts at day 5 revealed that Uex expression was noticeably reduced in the *uex* knockdown samples. Concurrent overexpression of a full-length *uex* transgene in the *uex* RNAi background elevated total Uex expression.

(D) S2 cells were subjected to immunofluorescence staining with anti-PRL-1 (red) and anti-Uex (green), and localization of Uex and PRL-1 on cell membranes was observed (arrows).

(E–G) Loss of Uex function (*elav/+; UAS-uex-IR/+*) in the fly nervous system results in abnormal wing posture (F), compared to the control (E).

Wing held-up phenotype was restored with concurrent *UAS-uex* expression (*elav-GAL4/+; UAS-uex-IR/UAS-uex*) (C and G). Scale bar, 100 μm in (D) and 37 μm in (G).

See also Figures S4 and S5.

Given the abnormal wing phenotype induced by CO_2 in *PRL-1* mutant flies, and a direct interaction between PRL-1 and Uex, this prompted us to examine the *uex* phenotype. As *uex* mutations generated with CRISPR/Cas9 method were larval lethal (Figure S5B), we employed an alternative RNAi approach. An array of different tissue-specific GAL4 drivers was used to evaluate the Uex knockdown phenotype (Figure S4D). As compared to the control (Figure 5E), only knockdown of *uex* in the nervous system (*elav > uex-IR*) led to the held-up wing phenotype after eclosion (Figure 5F), which was identical to the phenotype observed in the *PRL-1* mutant (Figure 1D). Western blot with brain extracts at day 5 after eclosion revealed that Uex expression was noticeably reduced in the *uex* knockdown samples (Figure 5C). Concurrent overexpression of a full-length *uex* transgene in the *uex* RNAi background elevated total Uex expression (Figure 5C) and rescued the wing phenotype (Figure 5G).

Uex Functions Downstream of PRL-1

To clarify a potential PRL-1/Uex interrelationship, we examined Uex expression in *PRL-1* mutant flies. In the *wt*, the Uex protein was detected as a doublet with a major band of 94 kDa and a faint band of 90 kDa (Figure 6A). We assume that the lower-molecular-weight band was the depredated product of the 94-KDa Uex protein. The

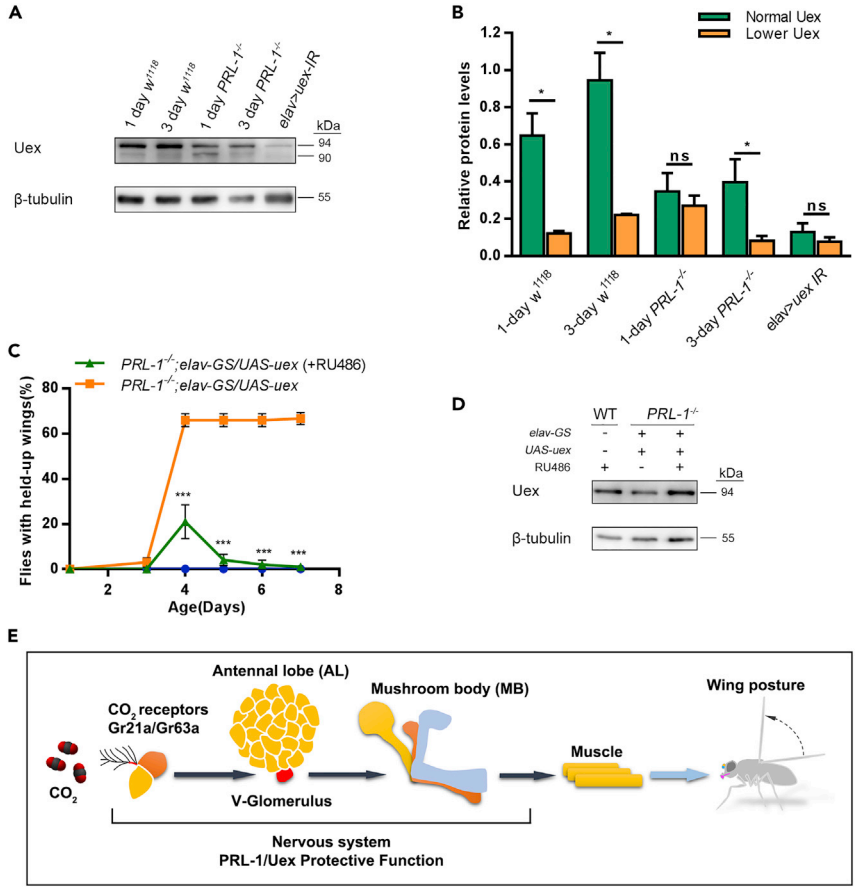

Figure 6. Uex Functions Downstream of PRL-1

(A) Western blot analysis of protein levels of Uex in day-1 and day-3-old controls, *PRL-1* mutants, and Uex knockdown flies. Uex was detected as a doublet in the brains, with a major 94-kDa band and a fairly weak band of 90 kDa. The lower band could be a degraded protein product.

(B) The statistical analysis of the western blot results from triple experiments, Data are expressed as means ±SD. *$p < 0.05$.

(C) Conditionally induced overexpression of *uex* by RU486 with *elav-Gal4* GeneSwitch was observed in the adult nervous system. The expression of Uex was induced with 0.5 mg/mL RU486 in experimental groups for 2 days, and all flies were exposed with 20 s CO_2 on day 3. Within the next 24 h, the percentages of wing held-up flies were analyzed.

(D) The elevated Uex expression drastically prevented CO_2-induced wing phenotype, and the initial wing held-up phenotype (4 day) was completely reversed over the next few days. Data are expressed as means ± SD. ***$p < 0.001$. $n = 20$ for all groups.

(E) The diagram depicts the proposed protective functions of PRL-1/Uex in the nervous system in response to CO_2 stimulation.

expression levels of the Uex protein were significantly decreased in the absence of PRL-1 (Figure 6B). The lower-molecular-weight band was obvious in the newly hatched *PRL-1* mutant flies (day 1 after eclosion). However, this lower band almost disappeared in older animals (day 3) (Figures 6A and 6B). It appeared that in the absence of PRL-1, approximately one-third of the Uex protein started to degrade from day 1. At day 3, the lower band was almost undetectable but the full-length Uex band remained unchanged. This observation may explain the reason why 3-day-old mutant flies were more responsive to CO_2 exposure (Figure S1A).

Based on these data, we propose that in *wt* animals, the neuroprotective role of PRL-1 against CO_2 challenge depends on Uex. We reason that although Uex levels are down-regulated in the absence of PRL-1, this Uex level is higher than that of *uex* RNAi knockdown (Figure 6A, *elav > uexIR*) and the wing phenotype is not observed in newly hatched adults (Figure 1A). Upon CO_2 exposure, the compromised Uex levels in the nervous system could not antagonize the effect of the stimuli, resulting in the held-up wing phenotype.

In this scenario, the ectopic expression of *uex* in *PRL-1* mutants should block the CO_2-induced wing phenotype. A conditional RU486-dependent *elav-GAL4* (GeneSwitch) (Osterwalder et al., 2001) was employed to induce tissue-specific expression of *uex* in *PRL-1* mutants. As RU486 was fed to the newly hatched flies, the Uex protein was elevated in the brains (day 5, Figure 6D). Consistent with our compromised Uex hypothesis, the increased Uex expression comprehensively prevented the CO_2-induced wing phenotype with only about 20% of the flies showing the phenotype, when compared with the 70% of unfed flies (Figure 6C). Interestingly, any initial held-up wing phenotype (day 4) observed in RU486-fed flies was completely reversed over the following few days (Figure 6C). This experiment clearly demonstrates that Uex acts downstream of PRL-1 and protects the nervous system against CO_2 challenge. Ectopic expression of *uex* in the nervous system not only prevents the wing phenotype development but also reverses the phenotype in individual mutant flies.

DISCUSSION

In this study we demonstrate that in *Drosophila* adult flies, PRL-1 functions in the nervous system and prevents CO_2-induced neural defects manifested by a held-up wing phenotype. Our genetic rescue data strongly indicate that it is defects in the nervous system that cause the CO_2-induced wing phenotype in *PRL-1* mutant flies. No obvious defects in muscles were observed (Figure S2), and ectopic expression of PRL-1 in muscles alone could not rescue the phenotype. The CO_2-induced wing phenotype was triggered initially by the signals from the CO_2 sensory neurons. Specific knockdown of CO_2 receptor protein Gr21a in these neurons fully prevented the wing phenotype in the *PRL-1* mutants.

The holding-up of wings in the fly is a behavioral output signal usually indicating avoidance or acceptance of a stimulus. Olfactory CO_2 detection via the receptors Gr21a and Gr63a in the CO_2-reseponsive neurons mediates avoidance (Jones et al., 2007), whereas E409 neurons, a population of taste neurons, have been identified to mediate taste acceptance in flies that are attracted to CO_2 in solution (Fischler et al., 2007). This indicates that compartmentalization of CO_2 detection may allow *Drosophila* to distinguish local versus global CO_2 levels and finely regulate behavior. In our study, the *PRL-1* mutant flies retained normal responses to anesthesia including N_2, volatile ether, and CO_2. However, without PRL-1 protection, the processing of olfactory CO_2 stimulation was rendered defective, resulting in a permanent holding up of wings. Many other gene mutations such as *Apterous* (Weihe et al., 2001) and *Beadex* (Kairamkonda and Nongthomba, 2014; Biryukova et al., 2009) could produce held-up curled wings. *Parkin* and *pink* mutants also exhibit held-up or drooped wing phenotype due to muscle defects (Yang et al., 2006; Fernandes and Rao, 2011). Such a hold up differs in nature to the *PRL-1* case. Here we report that the occurrence of a held-up wing phenotype is caused by gene disruption, which might regulate neuronal homeostasis, and this demonstrates that olfactory CO_2 stimulation is associated with the risk of neurological dysfunction for which PRL-1 provides defense.

Neural expression of shi^{ts1} in *wt* background provides a valuable clue to understand the rationale behind the held-up wing phenotype. Within the recovery time (about 10 min) when flies were shifted back from the non-permissive temperature (29°C) to the permissive temperature (25°C), they exhibited a held-up wing phenotype, which was reminiscent of that observed in *PRL-1* mutant flies induced by CO_2 exposure, except that in this case it was transient rather than permanent. As the nervous system is only partially functional during the period of recovery, we conclude that CO_2-induced held-up wing phenotype in *PRL-1* mutant flies is most likely due to neural dysfunction. Our data showed that expression of shi^{ts1} in motor neurons (*D42-GAL4*) also induced wing hold-up phenotype, although with a lower penetrance. This could simply be due to the lower-level expression of shi^{ts1} in motor neurons.

There are three members of the mammalian PRL family. *Drosophila* PRL-1 shares high similarities (74%–76%) to all three mPRLs (Zeng et al., 2000; Lin et al., 2013). Bai et al. recently reported that PRL1/PRL2 double knockout mice were embryonic lethal. However, $PRL1^{-/-}/PRL2^{+/-}$ and $PRL1^{+/-}/PRL2^{-/-}$ mice are viable, suggesting that there is a functional redundancy between PRL1 and PRL2 (Bai et al., 2016). Mice deficient for PRL3 were grossly normal (Zimmerman et al., 2013). Our study reveals that the *PRL-1* mutant flies are viable and fertile, even when they occurred with held-up wings, which negated flight for their entire lifespan. Using molecular mapping, we found that PRL-1 was enriched in the V-glomeruli of the AL and the MB of the *Drosophila* brain. We demonstrate that PRL-1 functions to protect against olfactory CO_2 stimulation. Our study suggests that *Drosophila* PRL-1 might not be critically required for survival, but essential for the maintenance of the neural homeostasis under stress conditions.

In mammals, PRL-2 regulates intracellular magnesium levels by forming a functional heterodimer with the magnesium transporter CNNM3 (Hardy et al., 2015). However, a substrate-trapping assay revealed that the mutation of catalytic cysteine to serine, or the mutation of aspartic acid to alanine in the WPD motif of PRL-2, did not lead to increased complex formation but to a strong reduction in the binding between the two proteins. This suggests that a catalytically active form of PRL-2 is still crucial for its association with CNNM3. We have also obtained a similar result by using substrate trapping mutants in analyzing the binding of *Drosophila* PRL-1 to Uex and have confirmed that Uex is not a typical phosphorylated substrate for PRL-1. The physiological substrate of PRl-1 is still unknown. It is possible that *Drosophila* PRL1 acts both as a trigger of Uex for a particular neuronal pathway and as a lipid phosphatase to maintain an active conformation for additional functions, for example, to control magnesium homoeostasis through the PRL-1/Uex complex.

The CBS pair domain of the magnesium transporter MgtE acts as a magnesium sensor and regulates the gating of the activity of the magnesium-transporting pore (Hattori et al., 2007). To confirm that Uex protein does indeed bind PRL-1 through its CBS domain, we designed a guide RNA targeted to the CBS domain using CRISPR/Cas9 method. We got many mutants, but most of them were lethal. Only one of them was homozygous viable, named uex^{7-7-1}, which caused two amino acids to be turned to one amino acid in the CBS domain (Figure S5C). The disrupted Uex protein extracted from this single mutant line exhibited decreased binding to PRL-1, as revealed by a GST pull-down assay (Figure S5D).

In our study, loss of PRL-1 clearly decreased the expression of Uex. Direct knockdown of Uex resulted in the same wing phenotype as observed in the *PRL-1* mutants, whereas abnormal wing posture in *PRL-1* mutants could be restored by rescuing Uex expression, particularly in the nervous system. However, we found that the loss of Uex causes fly lethality. In the mouse model, knockout of PRL-1 or PRL-2 only affects the related CNNMs protein. In this case, because the CNNM family has four members, the partial degradation of only one CNNM member is not enough to cause lethality. However, double mutants of PRL-1 and PRL-2 are clearly enough to decrease CNNMs' protein expression, which then causes the lethality of the mouse. Mg^{2+} acts as a physiological Ca^{2+} antagonist for blocking the excitatory N-methyl-D-aspartate receptors in the CNS (Zito and Scheuss, 2009; Iseri and French, 1984) and has therefore been suggested as a possible means of resolving muscle rigidity and spasms in cases of tetanus (Ceneviva et al., 2003). In humans, mutations in CNNM2 cause seizures and mental retardation in patients with hypomagnesemia (Arjona et al., 2014). CNNM4 can regulate Ca^{2+} influx during sperm capacitation (Yamazaki et al., 2016). Although we were unable to measure the Mg^{2+}homeostasis status in the *PRL-1* mutants and *uex*-IR flies, enhanced Ca^{2+} activities were induced in the *PRL-1* mutants. It would be possible that, if the cations, either magnesium or calcium, were added to the flies, this would affect the CNS homeostasis in *Drosophila*.

We have achieved a complete rescue in the *Drosophila* PRL-1 wing phenotype by using either hPRL-1 or hPRL-2 transgenic flies. This may imply that human PRL phosphatases are poised to function in a way similar to that we have shown for neuroprotection in *Drosophila*. Human PRL-3 has been demonstrated to dephosphorylate lipids and to affect phosphatidylinositol 3-kinase (PI3K) signaling (Wang et al., 2007). *Drosophila* PRL-1 is also thought to affect phosphoinositide-dependent PI3K-PTEN signaling loop, leading to the spatially restricted synapse formation (Urwyler et al., 2019). For an unknown reason we have found it a technical difficulty to produce hPRL-3 transgenic flies for the rescue experiment. Weather PRL1 in *Drosophila* acts as a lipid PTP (protein tyrosine phosphatase) in CO_2 neural circuits remains to be illustrated.

In conclusion, we have identified a novel neural protective function of PRL-1/Uex (Figure 6E). In the absence of PRL-1, Uex expression levels are down-regulated. Upon CO_2 exposure, the receptors in the CO_2 sensory neuron send signals to the nervous system, triggering behavioral responses. The AL region of the brain in *PRL-1* mutants exhibits hypersensitive Ca^{2+} responses to CO_2 exposure. This hypersensitivity combined with low levels of Uex leads to neural dysfunction, resulting in the held-up wing phenotype. Although primarily recognized for PRL's oncogenic properties in mammals, here we highlight its neuroprotective role in the nervous system, particularly in relation to the CO_2 sensory motor pathway in *Drosophila*. Our study implies that PRLs may retain a similar neuroprotective function in humans. It also comes to our attention that the phenomena of neurological dysfunction induced by CO_2 insult in *PRL-1* mutants resembles the post-traumatic stress disorder in humans, in which transient severe unfavorable stimulating factors cause ongoing neurological dysfunction. Further investigations are needed to confirm the correlation.

Limitations of the Study

Although we have revealed a Prl-1-Uex complex-based neuroprotective mechanism in which Prl-1 protects against nervous system insult related to olfactory CO2 stimulation, any human neuroprotective mechanisms related to the issue of CO_2 toxicity, particularly those relating to olfactory pathways, have yet to be elucidated. It is true that in human brain disorders such as Parkinson and Alzheimer diseases, there is profound olfactory disorder in odor threshold detection, odor memory, or odor identification often occurring before disease onset. These are often associated with aspects of limb dysfunction. However, the reasons and mechanisms of such still remain unknown. The potential role of hPRL-1 in this process requires further study.

METHODS

All methods can be found in the accompanying Transparent Methods supplemental file.

SUPPLEMENTAL INFORMATION

Supplemental Information can be found online at https://doi.org/10.1016/j.isci.2019.07.026.

ACKNOWLEDGMENTS

We thank Jun Ma, Hao Wang, and Lijun Kang for helpful suggestions on data analysis. We give special thanks to Qi Zeng for the encouragement to initiate this study. We thank Chris Wood for discussions on the manuscript. We thank Jiangqu Liu for GCaMP flies and the Bloomington *Drosophila* Stock Center and Tsinghua *Drosophila* Stock Center for providing the fly stocks. This work was supported by National Key R&D Program of China (2018YFC1004900) and the National Basic Research Program of China (2013CB945600, X.Yang.).

AUTHOR CONTRIBUTIONS

Y.X. and X.Yang. conceived the idea of the project, designed the overall experiments, and supervised the overall research project. P.G. and X.X. contributed to designing the experiments and performed the experiments. F.W., X.Yuan., Y.T., B.Z., H.Z., and D.Y. contributed to the experiments. W.G. and Z.G. contributed to project discussion and coordination. Y.X., X.Yang., P.G., and X.X. wrote the manuscript.

DECLARATION OF INTERESTS

The authors declare that they have no conflict of interest.

Received: April 29, 2019
Revised: July 10, 2019
Accepted: July 16, 2019
Published: September 27, 2019

REFERENCES

Al-Aidaroos, A.Q.O., and Zeng, Q. (2010). PRL-3 phosphatase and cancer metastasis. J. Cell. Biochem. *111*, 1087–1098.

Arjona, F.J., De Baaij, J.H., Schlingmann, K.P., Lameris, A.L., Van Wijk, E., Flik, G., Regele, S., Korenke, G.C., Neophytou, B., et al. (2014). CNNM2 mutations cause impaired brain development and seizures in patients with hypomagnesemia. PLoS Genet. *10*, e1004267.

Badre, N.H., Martin, M.E., and Cooper, R.L. (2005). The physiological and behavioral effects of carbon dioxide on Drosophila melanogaster larvae. Comp. Biochem. Physiol. A Mol. Integr. Physiol. *140*, 363–376.

Bai, Y., Zhou, H.M., Zhang, L., Dong, Y., Zeng, Q., Shou, W., and Zhang, Z.Y. (2016). Role of phosphatase of regenerating liver 1 (PRL1) in spermatogenesis. Sci. Rep. *6*, 34211.

Bassett, A., and Liu, J.L. (2014). CRISPR/Cas9 mediated genome engineering in Drosophila. Methods *69*, 128–136.

Bassett, A., Tibbit, C., Ponting, C., and Liu, J.L. (2013). Highly efficient targeted mutagenesis of Drosophila with the CRISPR/Cas9 system. Cell Rep. *4*, 220–228.

Bessette, D.C., Qiu, D., and Pallen, C.J. (2008). PRL PTPs: mediators and markers of cancer progression. Cancer Metastasis Rev. *27*, 231–252.

Biryukova, I., Asmar, J., Abdesselem, H., and Heitzler, P. (2009). Drosophila mir-9a regulates wing development via fine-tuning expression of the LIM only factor, dLMO. Dev. Biol. *327*, 487–496.

Campbell, A.M., and Zhang, Z.Y. (2014). Phosphatase of regenerating liver: a novel target for cancer therapy. Expert Opin. Ther. Targets *18*, 555–569.

Ceneviva, G.D., Thomas, N.J., and Kees-Folts, D. (2003). Magnesium sulfate for control of muscle rigidity and spasms and avoidance of mechanical ventilation in pediatric tetanus. Pediatr. Crit. Care Med. *4*, 480–484.

Couto, A., Alenius, M., and Dickson, B.J. (2005). Molecular, anatomical, and functional organization of the Drosophila olfactory system. Curr. Biol. *15*, 1535–1547.

Diamond, R.H., Cressman, D.E., Laz, T.M., Abrams, C.S., and Taub, R. (1994). PRL-1, a unique nuclear protein tyrosine phosphatase, affects cell growth. Mol. Cell. Biol. *14*, 3752–3762.

Dijken, F.R.V., Sambeek, M.J.P.W.V., and Scharloo, W. (1977). Influence of anaesthesia by

carbon dioxide and ether on locomotor activity in Drosophila melanogaster. Experientia *33*, 1360–1361.

Fernandes, C., and Rao, Y. (2011). Genome-wide screen for modifiers of Parkinson's disease genes in Drosophila. Mol. Brain *4*, 17.

Fischler, W., Kong, P., Marella, S., and Scott, K. (2007). The detection of carbonation by the Drosophila gustatory system. Nature *448*, 1054–U9.

Funato, Y., Yamazaki, D., Mizukami, S., Du, L., Kikuchi, K., and Miki, H. (2014). Membrane protein CNNM4-dependent Mg2+ efflux suppresses tumor progression. J. Clin. Invest. *124*, 5398–5410.

Guerenstein, P.G., Christensen, T.A., and Hildebrand, J.G. (2004). Sensory processing of ambient CO 2 information in the brain of the moth Manduca sexta. J. Comp. Physiol. A *190*, 707–725.

Gungabeesoon, J., Tremblay, M.L., and Uetani, N. (2016). Localizing PRL-2 expression and determining the effects of dietary Mg 2+ on expression levels. Histochem. Cell Biol. *146*, 99–111.

Hardy, S., Uetani, N., Wong, N., Kostantin, E., Labbe, D.P., Begin, L.R., Mes-Masson, A., Miranda-Saavedra, D., and Tremblay, M.L. (2015). The protein tyrosine phosphatase PRL-2 interacts with the magnesium transporter CNNM3 to promote oncogenesis. Oncogene *34*, 986–995.

Hattori, M., Tanaka, Y., Fukai, S., Ishitani, R., and Nureki, O. (2007). Crystal structure of the MgtE Mg2+ transporter. Nature *448*, 1072–U13.

Iseri, L.T., and French, J.H. (1984). Magnesium - natures physiologic calcium blocker. Am. Heart J. *108*, 188–193.

Ji, H., Chun, Z., Cheng, D., Qiuyi, C., Andreas, W., Peter, M., Hiroaki, M., and Minmin, L. (2007). Detection of near-atmospheric concentrations of CO2 by an olfactory subsystem in the mouse. Science *317*, 953–957.

Jones, W.D., Cayirlioglu, P., Kadow, I.G., and Vosshall, L.B. (2007). Two chemosensory receptors together mediate carbon dioxide detection in Drosophila. Nature *445*, 86–90.

Kairamkonda, S., and Nongthomba, U. (2014). Beadex function in the motor neurons is essential for female reproduction in Drosophila melanogaster. PLoS One *9*, e113003.

Kitamoto, T. (2001). Conditional modification of behavior in Drosophila by targeted expression of a temperature-sensitive shibire allele in defined neurons. J. Neurobiol. *47*, 81–92.

Kosaka, T., and Ikeda, K. (2010). Possible temperature-dependent blockage of synaptic vesicle recycling induced by a single gene mutation in Drosophila. Dev. Neurobiol. *14*, 207–225.

Kwon, J.Y., Dahanukar, A., Weiss, L.A., and Carlson, J.R. (2007). The molecular basis of CO2 reception in Drosophila. Proc. Natl. Acad. Sci. U S A *104*, 3574–3578.

Lin, M.D., Lee, H.T., Wang, S.C., Li, H.R., Hsien, H.L., Cheng, K.W., Chang, Y.D., Huang, M.L., Yu, J.K., and Chen, Y.H. (2013). Expression of phosphatase of regenerating liver family genes during embryogenesis: an evolutionary developmental analysis among Drosophila, amphioxus, and zebrafish. BMC Dev. Biol. *13*, 18.

McMeniman, C., Corfas, R., Matthews, B., Ritchie, S., and Vosshall, L. (2014). Multimodal integration of carbon dioxide and other sensory cues drives mosquito attraction to humans. Cell *156*, 1060–1071.

Osterwalder, T., Yoon, K.S., White, B.H., and Keshishian, H. (2001). A conditional tissue-specific transgene expression system using inducible GAL4. Proc. Natl. Acad. Sci. U S A *98*, 12596–12601.

Pagarigan, K.T., Bunn, B.W., Goodchild, J., Rahe, T.K., Weis, J.F., and Saucedo, L.J. (2013). Drosophila PRL-1 is a growth inhibitor that counteracts the function of the Src oncogene. PLoS One *8*, e61084.

Sachse, S., Rueckert, E., Keller, A., Okada, R., Tanaka, N.K., Ito, K., and Vosshall, L.B. (2007). Activity-dependent plasticity in an olfactory circuit. Neuron *56*, 838–850.

Saha, S., Bardelli, A., Buckhaults, P., Velculescu, V.E., Rago, C., St Croix, B., Romans, K.E., Choti, M.A., Lengauer, C., Kinzler, K.W., and Vogelstein, B. (2001). A phosphatase associated with metastasis of colorectal cancer. Science *294*, 1343–1346.

Scott, K., Brady, R., Cravchik, A., Morozov, P., Rzhetsky, A., Zuker, C., and Axel, R. (2001). A chemosensory gene family encoding candidate gustatory and olfactory receptors in Drosophila. Cell *104*, 661–673.

Shusterman, D., and Avila, P.C. (2003). Real-time monitoring of nasal mucosal pH during carbon dioxide stimulation: implications for stimulus dynamics. Chem. Senses *28*, 595.

Stange, G., and Stowe, S. (1999). Carbon-dioxide sensing structures in terrestrial arthropods. Microsc. Res. Tech. *47*, 416–427.

Suh, G.S.B., Wong, A.M., Hergarden, A.C., Wang, J.W., Simon, A.F., Benzer, S., Axel, R., and Anderson, D.J. (2004). A single population of olfactory sensory neurons mediates an innate avoidance behaviour in Drosophila. Nature *431*, 854.

Takano, S., Fukuyama, H., Fukumoto, M., Kimura, J., Xue, J.H., Ohashi, H., and Fujita, J. (1996). PRL-1, a protein tyrosine phosphatase, is expressed in neurons and oligodendrocytes in the brain and induced in the cerebral cortex following transient forebrain ischemia. Mol. Brain Res. *40*, 105–115.

Urwyler, O., Izadifar, A., Vandenbogaerde, S., Sachse, S., Misbaer, A., and Schmucker, D. (2019). Branch-restricted localization of phosphatase Prl-1 specifies axonal synaptogenesis domains. Science *364*, 454.

Vosshall, L.B., and Stocker, R.F. (2007). Molecular architecture of smell and taste in Drosophila. Annu. Rev. Neurosci. *30*, 505–533.

Wang, H., Quah, S.Y., Dong, J.M., Manser, E., Tang, J.P., and Zeng, Q. (2007). PRL-3 down-regulates PTEN expression and signals through PI3K to promote epithelial-mesenchymal transition. Cancer Res. *67*, 2922–2926.

Wang, J.W., Wong, A.M., Flores, J., Vosshall, L.B., and Axel, R. (2003). Two-photon calcium imaging reveals an odor-evoked map of activity in the fly brain. Cell *112*, 271–282.

Weihe, U., Milan, M., and Cohen, S.M. (2001). Regulation of Apterous activity in Drosophila wing development. Development *128*, 4615–4622.

Yamazaki, D., Miyata, H., Funato, Y., Fujihara, Y., Ikawa, M., and Miki, H. (2016). The Mg2+ transporter CNNM4 regulates sperm Ca2+ homeostasis and is essential for reproduction. J. Cell Sci. *129*, 1940–1949.

Yang, Y.F., Gehrke, S., Imai, Y., Huang, Z.N., Ouyang, Y., Wang, J.W., Yang, L.C., Beal, M.F., Vogel, H., and Lu, B.W. (2006). Mitochondrial pathology and muscle and dopaminergic neuron degeneration caused inactivation of Drosophila Pink1 is rescued by Parkin. Proc. Natl. Acad. Sci. U S A *103*, 10793–10798.

Zeng, Q., Hong, W., and Tan, Y.H. (1998). Mouse PRL-2 and PRL-3, two potentially prenylated protein tyrosine phosphatases homologous to PRL-1. Biochem. Biophys. Res. Commun. *244*, 421–427.

Zeng, Q., Si, X.N., Horstmann, H., Xu, Y., Hong, W.J., and Pallen, C.J. (2000). Prenylation-dependent association of protein-tyrosine phosphatases PRL-1,-2, and-3 with the plasma membrane and the early endosome. J. Biol. Chem. *275*, 21444–21452.

Zimmerman, M.W., Homanics, G.E., and Lazo, J.S. (2013). Targeted deletion of the metastasis-associated phosphatase Ptp4a3 (PRL-3) suppresses murine colon cancer. PLoS One *8*, e58300.

Zito, K., and Scheuss, V. (2009). NMDA receptor function and physiological modulation. In Encyclopedia of Neuroscience, L.R. Squire, ed. (Academic Press), pp. 1157–1164.

ISCI, Volume *19*

Supplemental Information

A Novel Neuroprotective Role of *Phosphatase of Regenerating Liver-1* against CO_2 Stimulation in *Drosophila*

Pengfei Guo, Xiao Xu, Fang Wang, Xin Yuan, Yinqi Tu, Bei Zhang, Huimei Zheng, Danqing Yu, Wanzhong Ge, Zhefeng Gong, Xiaohang Yang, and Yongmei Xi

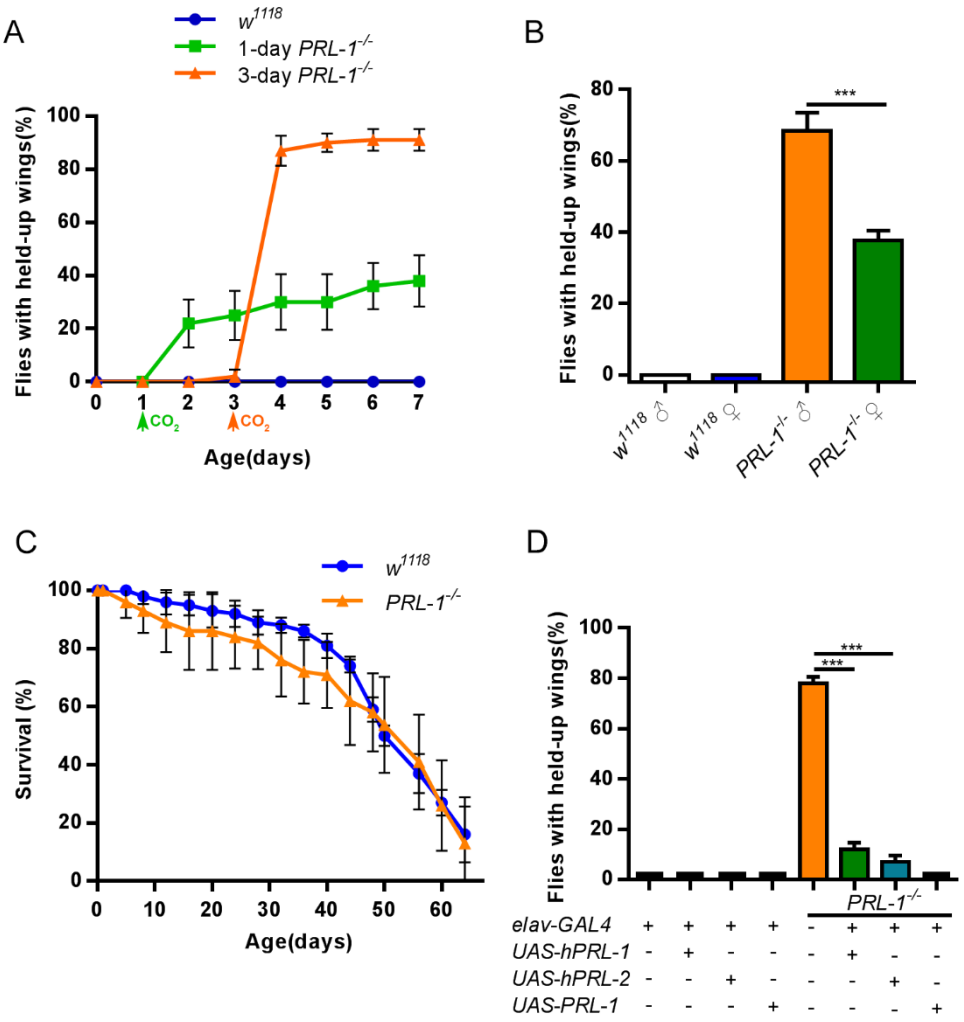

Figure S1. Held-up Wing Phenotype in *PRL-1* Mutant Flies. Related to Figure 1.

(A) Age-dependent occurrences of wing phenotype in *PRL-1* mutants. 1-day-old and 3-day-old *wt* or *PRL-1* mutants treated with CO_2. Day-3 mutants showed more sensitivity to CO_2 stimulation. (B) The mutant male flies showed more response to CO_2 treatment. *PRL-1* male mutant animals displayed more prevalent held-up wings than the female (over 70% as compared to nearly 40%). (C) Quantification of survival rates for *wt* and *PRL-1* mutant flies with wing phenotype. *PRL-1* mutant flies show similar survival rates as control animals. (D) Two human homologs, hPRL-1 and hPRL-2, expressed in the nervous system could fulfill *Drosophila* PRL-1 function and effectively rescue the wing phenotype.

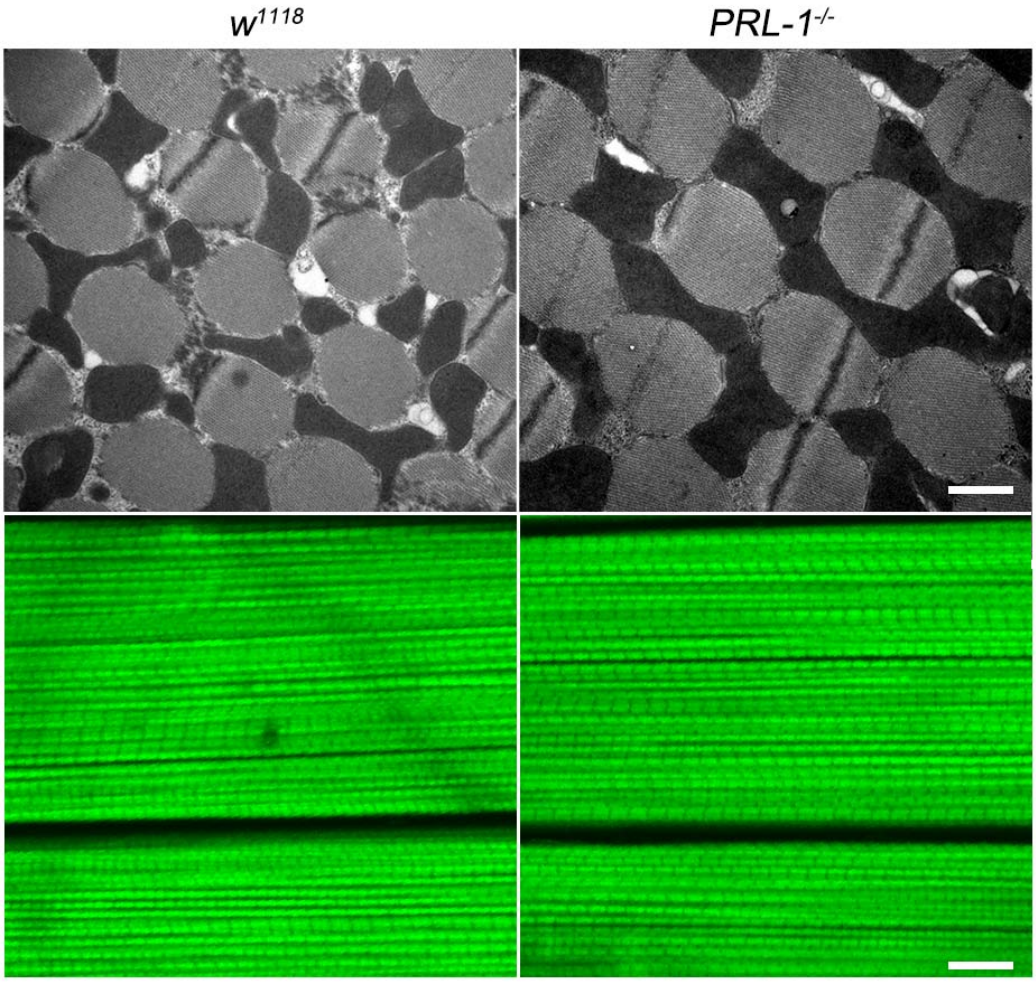

Figure S2. Transmission Electrical Microscope Images of Indirect Flight Muscle. Related to Figure 2.

Examination of indirect flight muscle (IFM) by Transmission Electrical Microscopy and Phalloidin staining showed no obvious differences between the *wt* and the mutants. Based on these observations we conclude that PRL-1 plays an important protective role in the nervous system. The held-up wing phenotype induced by CO_2 exposure was caused by defective neuronal function in the absence of PRL-1. Indirect flight muscle images of *wt* and *PRL-1* mutant flies are shown. Scale bars: 1 μm.

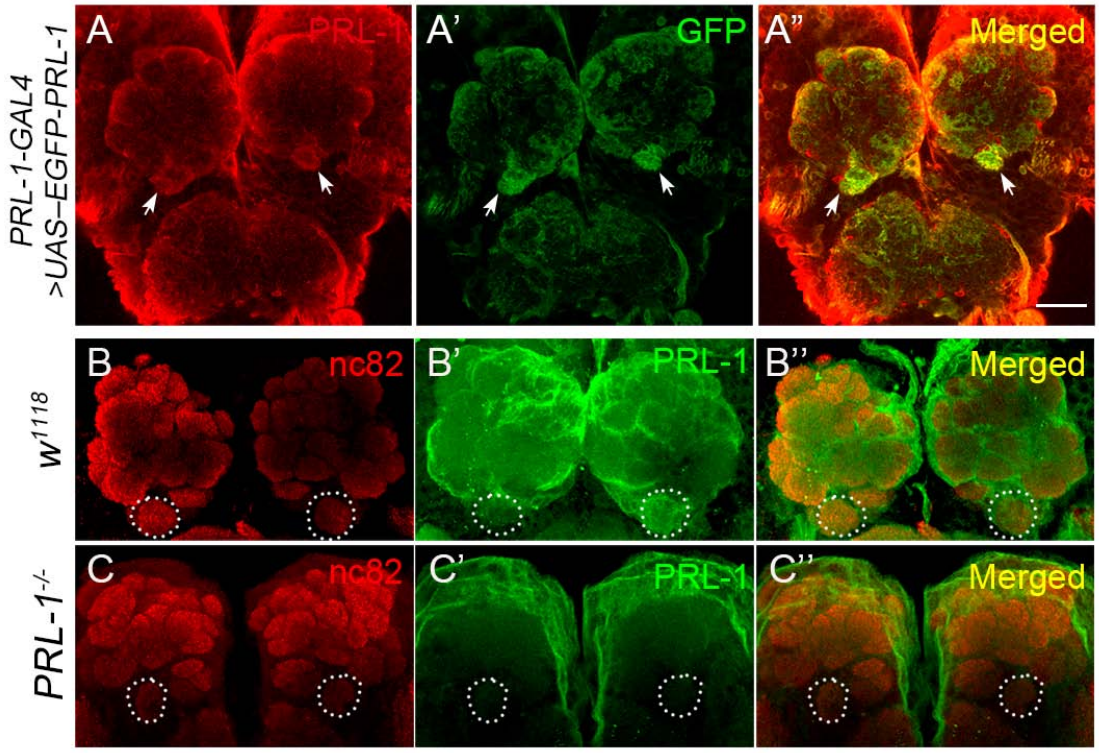

Figure S3. Detection of PRL-1 and PRL-1-GAL4 Expression in the Adult Brains. Related to Figure 3.

(A-A") Immunofluorescent staining of transgenic flies with over expression of EGFP-PRL-1 driven by *PRL-1*-GAL4. The anti-PRL-1 and anti-GFP staining showed similar patterns in the adult brains, in which they both had signal at the antennal lobe (AL) and V-Glomeruli (white arrows). (B-B", C-C") Staining of wild-type and *PRL-1* null mutant adult brains using PRL-1 antibody, showed PRL-1 expression in the antennal lobe, particularly in the V-Glomeruli (B-B"), which was undetectable in the null mutant (C-C").

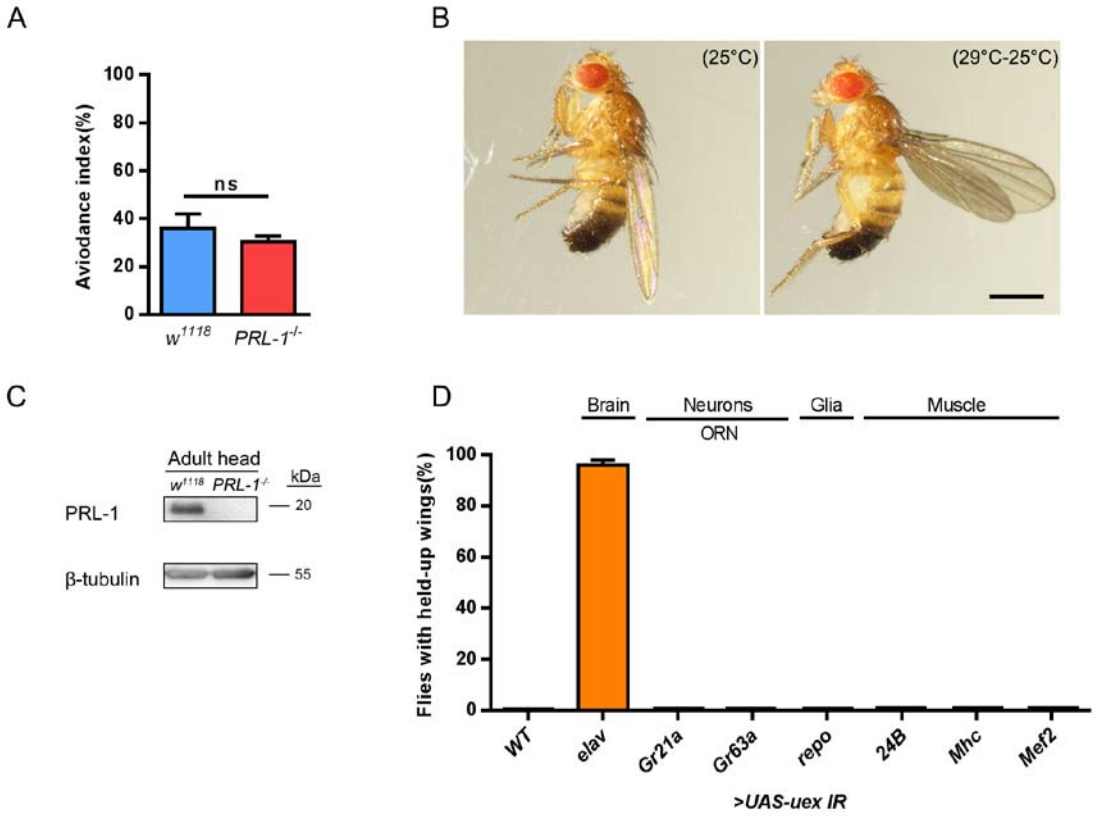

Figure S4. Exploration of the Possible Causes for the Wing Phenotype. Related to Figure 4 and Figure 5.

(A) Compared with wild type flies, *PRL-1* mutants exhibit no significant difference in CO_2–induced avoidance behaviour in a T-maze test. Data are expressed as means ± SD. ***p<0.001, ns, not significant. (B) When shifted back from non-permissive temperature to the permissive temperature (29 ^{o}C to 25 ^{o}C), flies expressing *shi^{ts1}* in the nervous system exhibited a transient held-up wing phenotype. (C) Western blot of adult brain extracts from *wt* and *PRL-1* mutant animals. Lysates were probed with anti-PRL-1 and anti-tubulin. Data are expressed as means ± SD. ***p<0.001. Scale bar: 80μm. (D) *uex* RNAi knockdown was tested with a battery of *GAL4* lines: *elav-GAL4* (pan-neuronal), *Gr21a-GAL4* and *Gr63a-GAL4* (olfactory receptor neurons), *repo-GAL4* (glia), *24B-GAL4*, *Mhc-GAL4* and *Mef2-GAL4* (muscles). (n=60 each group). Only specific knockdown of *uex* in the nervous system led to held-up wing phenotype. Data are expressed as means ± SD.

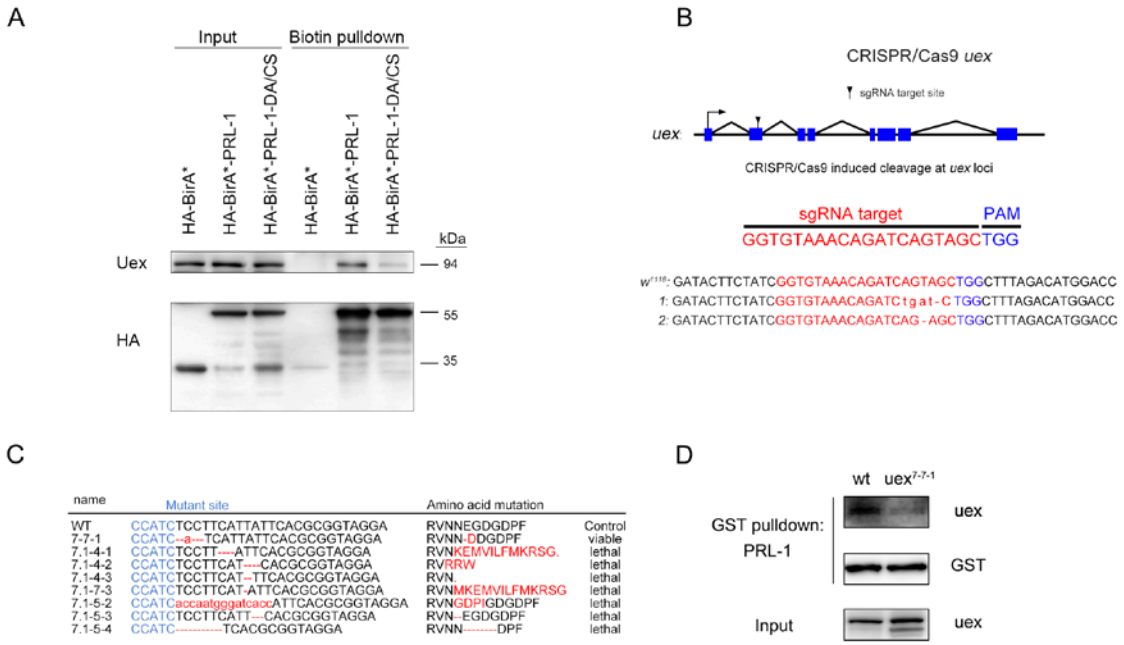

Figure S5. The Analysis of the Interaction Between PRL-1 and Uex. Related to Figure 5.

(A) Biotin Pull-down experiment confirms the interaction between PRL-1 and Uex. A UAS-HA-BirA tag was constructed with either empty or HA-tagged PRL-1 (WT or D77A/C109S mutant), then injected into fly germline cells to make stable transgenic flies. Tubulin-Gal4 was used to drive these transgenic lines. Lysates were extracted from these progenies for biotin pulldown assay. (B). Generation of *uex* mutant by using CRISPR/Cas9 system, the target of *uex* gRNA was located in the second exon. Two mutant lines were obtained with mutation in the gRNA target sequence, which produced in-frame shifted and stop codon in *uex* locus. (C) Mutated CBS domain of Uex was generated by constructing CBS domain target gRNA and using CRISPR/Cas9 method to obtaine CBS domain loss-of-function *uex* allels. (D) GST pulldown assay showed that Uex with the mutated CBS domain lost its physical interaction with PRL-1..

Transparent Methods

Fly Strains and Genetics

The following transgenic flies were used: (1) *elav-GAL4*, (2) *Tubulin-GAL4*, (3) *Repo-GAL4*, (4) *TH-GAL4*, (5) *Orco-GAL4*, (6) *Or47b-GAL4*, (7) *Gr21a-GAL4*, (8) *Gr63a-GAL4*, (9)*Mef2-GAL4*, (10)*MHC-GAL4*, (11) *MB247-GAL4*, (12) *OK107-GAL4*, (13) *GF-GAL4*, (14) *D42-GAL4*, (15) *24B-GAL4*, (16) *Vglut-GAL4*, (17) *elav-GeneSwitch-GAL4*, (18)*UAS-shi^{ts1}*,(19)*UAS-Gr21a-IR,* (20) *UAS-mCD8::GFP*, (21) *UAS-GCaMP6.0*,(22) *UAS-uex-IR*. All fly genetics and manipulations followed standard protocols.

Generation of *PRL-1* and *uex* Mutant by CRISPR/Cas9 Methods

PRL-1 and *uex* mutations were generated by CRISPR/Cas9 system according to Bassett et al, 2013 and 2014 (Bassett and Liu, 2014; Bassett et al., 2013). Two gRNA sequences for the *PRL-1* gene and a gRNA sequence for *uex* gene were designed using CRISPR Optimal Target Finder (http://targetfinder.flycrispr.neuro.brown.edu/). The gRNAs were injected into wild-type *Drosophila* embryo respectively with synthesized Cas9 mRNA. The sequences of two distinct *PRL-1* gRNA target sites are GGTTATGTCTGATGGTCGATCGG and GGTTAAGGCTTACACGATTATGG. The gRNA target for *uex* gene is GGTGTAAACAGATCAGTAGCTGG. The F_0 flies' genotype was sequenced using specific primers that were flanking the gRNA target region. F_1 flies were generated by crossing F_0 with a balancer line and their genotypes were sequence analyzed for the mutation. F_2 was generated by crossing the virgin balancer line with male F_1, which had been previously confirmed by sequence analyses. Their later generations were used as mutants for further experiments.

Generation of Transgenic Flies

PRL-1, EGFP-PRL-1, uex, hPRL-1, and hPRL-2 were amplified using the following primers :

EGFP-PRL-1: ATTCGTTAACAGATCTGCATGGTGAGCAAGGGCGAGG and

TCACAAAGATCCTCTAGAGCTATTGCACAGAACATGAAT;

PRL-1: CAAGAAGAGAACTCTGAATAATGAGCATCACCATGCGTC and

AGGTTCCTTCACAAAGATCCCTATTGCACAGAACATGAATTC;

hPRL-1:TACGCTGCTCATGGCGGAATGGCTCGAATGAACCGCC and

AGGTTCCTTCACAAAGATCCTTATTGAATGCAACAGTTGT;

hPRL-2: TACGCTGCTCATGGCGGAATGAACCGTCCAGCCCCT and

AGGTTCCTTCACAAAGATCCCTACTGAACACAGCAATGCC;

uex: AGAAGAGAACTCTGAATAATGAACACATATTTCATATC and

TTCCTTCACAAAGATCCTTAGGGCTTACTTTGCTTGCTCT. The PCR amplified sequences were cloned in a *pUAST-attb* plasmid and amplified by PCR. The *PRL-GAL4* was cloned from wild-type flies' genome with primers:

AATTGGGAATTCGTTAACATCACCATCCGTGTCTACCAAC and

ATCTTTCAGGAGGCGCGGCCACAATTACAAAAGCTGTTCT, then inserted in a *pW25-attb* plasmid, which flanked the *GAL4* sequence with both the 5' and 3' flanking regions of the *PRL-1* gene. All constructs were integrated into a single *attP* docking site, *VK33* on chromosome 3L, using common *phiC31* site-specific integration, as previously described by Matthew P Fish(Fish et al., 2007).

Antibody Generation

Full-length cDNA of *PRL-1*, and N-terminal 300bp cDNA of *uex* were cloned into a *pGEX-4T-1* expression vector and transformed into BL21 Competent *E.coli* cells to generate a fusion protein. The GST-fusion protein was affinity purified using Sepharose-4B beads (GE Healthcare). The polyclonal antibody was obtained via immunizing rabbits or guinea pigs. Animal experiments were conducted in accordance with the Guidelines for the Care and Use of Laboratory Animals of Zhejiang University.

Immunofluorescence Staining

Immunofluorescence staining of the adult brains and S2 cells were conducted as previously described (Riemensperger et al., 2011). The following primary antibodies were used: rabbit anti-PRL-1, 1:500 (this study); rabbit anti-Uex, 1:500; guinea pig anti-Uex, 1:500; chicken anti-GFP, 1:2000 (Abcam); mouse anti-nc82, 1:50 (DSHB); DAPI (1μg/ml; Sigma-Aldrich); rat

anti-Elav, 1:50 (DSHB).

CO_2 Treatment and T-maze Assay

In each experiment, *wt* or mutant flies in different age groups (20 flies per vial, 9 vials per group, n=180) were subjected to CO_2 under a flow of 5L/min for 20 sec. Non-CO_2-treated groups served as controls. All flies with a held-up wing phenotype were counted within 24 hours. For the T-maze experiment, we connected the T-maze with two empty vials, which were attached to a mini pump. About 50 flies of mixed gender were transferred into the T-maze by first placing them into an empty plastic centrifuge tube and tapping them into the elevator of the T-maze. While flies were in the elevator, an empty tube was filled full of CO_2 for 5L/min 20 sec and considered as conditioned tube. We attached the conditioned tube and another fresh tube separately to the T-maze and using mini pump to suck airflow from both sides of T-maze. The elevator containing flies was lowered, and the flies given one minute to choose between the two sides, after which the elevator was partially lifted to block any further choices. The number of flies in each tube was then counted (Suh et al., 2004) and the avoidance index (AI) was calculated.

Temperature Shift Experiment

The vials with the flies containing shi^{ts1} expressed in the nervous system were maintained at 25°C (n=60, 20 flies per vial) and shifted to 29°C in a water bath. The vials were then transferred back to 25°C. The animals with held-up wing phenotype were counted within the transition time (29 °C to 25°C, about 10 mins).

Muscle Preparations for Imaging

Five days after eclosion the thoraxes were isolated and dissected dorsal-ventrally and incubated in the 4% PFA to fix for further 20 min. The indirect flight muscles were removed and washed twice with PBS-T solution. Phalloidin-TRITC (Sigma) was used to stain the muscles before mounting in Vectashield.

Transmission Electron Microscopy

Half-thoraxes were dissected from adult males and prepared for electron microscopy using standard protocols. Thin sections were observed and photographed using a Hitachi H-7650

transmission electron microscope.

IP and GST Pull-down

S2 cells and fly tissues were lysed using TAP buffer (1% Triton, 50mMTris pH 8.0, 125mMNaCl, 5% Glycerol, 0.4% NP-40, 1.5mM$MgCl_2$, 1mMEDTA, 25mMNaF, and 1mMNa_3VO_4) supplemented with protease inhibitor (Roche, Laval, QC, Canada). For IP, 1mg of proteins was incubated with 1 µg of HA antibody (Abcam) and Protein A-agarose beads (Roche Applied Science) according to the manufacturer's protocol. The supernatants eluted from immunoprecipitated beads were loaded for Western blotting following standard protocols. For the GST pull-down assays, 500µg of proteins were incubated with glutathione Sepharose (GE Healthcare, Canada) for 3 hours.

Calcium Imaging

Sample preparation and calcium imaging were as described in Jones et al., (2007). The GCaMP indicator (*UAS-GCaMP6.0*) was driven by *elav-GAL4* in all neurons. CO_2 was delivered at a flow rate of 5L/min. The adult flies were fixed to a piece of Scotch tape with dorsal parts and wings. The maxillary palp also immobilized using a scotch tape strip. Imaging of Ca^{2+} was performed on Olympus confocal microscope with a x20 objective lens. Images were acquired at 1.42 frames per second. For quantitative analysis, Ca^{2+} image data was processed with Image J to determine fluorescence intensity. The initial 120 seconds of sequential images, occurring prior to the 20 second CO_2 stimulus, were subjectively selected and the average fluorescence intensity (F) was set as the basal level. Changes in fluorescence intensity (△F) in the images were calculated and △F/F was used to denote Ca^{2+} responses. Heat map images were generated using Matlab (Mathworks Inc., Natick, MA, USA) by setting the basal fluorescence level at zero

RU486 Induction Protocols and Held-up Wing Count.

Larvae were raised with standard fly food to the adult stage. Up to 10 mg/ml of RU486 (mifepristone, Sigma) was dissolved in ethanol. For adult feeding, RU486 was diluted 20-fold from the original concentration in ethanol and directly mixed with the adult food. The newly eclosed flies were starved for 3 hours on agar plates and transferred to 0.5 mg/ml RU486 food, where they resided for 48 hours before they were treated with high concentration of CO_2. After 24

hours recovery, a count was made of the flies which presented with held-up wings .

Statistics

All the raw data were analysed parametrically using excel and Graphpad Prism 5 software. The data was evaluated using a Two-tailed Student's t test. All data are presented as mean ±SD. *p< 0.05; **p< 0.01; ***p< 0.001, ns, not significant.